

SOLIDS
Electronic Properties

Frustrated Antiferromagnetism in the Sr_2YRuO_6 Double Perovskite

E. V. Kuz'min^a, S. G. Ovchinnikov^{a,*}, and D. J. Singh^b

^a*Kirenskiĭ Institute of Physics, Siberian Division, Russian Academy of Sciences,
Akademgorodok, Krasnoyarsk, 660036 Russia*

^b*Naval Research Laboratory, Washington, DC, USA*

*e-mail: sgo@iph.krasn.ru

Received December 9, 2002

Abstract—The spins of Ru^{5+} ions in Sr_2YRuO_6 form a face-centered cubic lattice with antiferromagnetic nearest neighbor interaction $J \approx 25$ meV. The antiferromagnetic structure of the first type experimentally observed below the Néel temperature $T_N = 26$ K corresponds to four frustrated spins of 12 nearest neighbors. In the Heisenberg model in the spin-wave approximation, the frustrations already cause instability of the antiferromagnetic state at $T = 0$ K. This state is stabilized by weak anisotropy D or exchange interaction I with the next-nearest neighbors. Low $D/J \sim I/J \sim 10^{-3}$ values correspond to the experimental T_N and sublattice magnetic moment values. © 2003 MAIK “Nauka/Interperiodica”.

1. INTRODUCTION

Like cuprates and manganates, perovskite-like ruthenates have been attracting much interest of researchers in recent years. Initially, this interest was caused by the discovery of exotic superconductivity in Sr_2RuO_4 [1]. This is the only oxide superconductor isostructural to cuprates that does not contain copper. Later, it was found that other ruthenates have very interesting magnetic and electric properties. Increasing x in the $\text{Sr}_{2-x}\text{Ca}_x\text{RuO}_4$ system results in a complex sequence of structural phase transitions, competition between ferromagnetic and antiferromagnetic exchange interactions, and the Mott–Hubbard metal–dielectric transition in Ca_2RuO_4 [2, 3]. Another ruthenate, SrRuO_3 , is the only metallic ferromagnet with $T_C \approx 165$ K and magnetization $m \approx 1.6\mu_B$ per Ru ion among $4d$ metal oxides [4, 5]. The Sr_2YRuO_6 double perovskite has an elpasolite structure, which can be obtained from SrRuO_3 by replacing each second Ru ion with nonmagnetic Y; below $T_N = 26$ K, the face-centered cubic (FCC) lattice of Ru^{5+} spins experiences ordering to produce an antiferromagnetic structure of the first type [6, 7]. In this structure, (001) ferromagnetic planes exhibit antiparallel ordering along the c axis.

One of the reasons for our interest in the magnetic properties of Sr_2YRuO_6 is its low T_N temperature and small value of the sublattice magnetic moment per ruthenium ion, $m = 1.85\mu_B$, compared with the exchange integral $J \approx 25$ meV and the nominal $m(S = 3/2) = 3\mu_B$ per Ru ion for the d^3 configuration of Ru^{5+} . The m value was measured by neutron diffraction [6, 7], and the J value was calculated theoretically [8].

Another reason for our interest in the double perovskite is the appearance of superconductivity with $T_c \approx 50$ K after doping it with copper [9, 10]. A study of a possible magnetic mechanism of superconductivity in this system requires understanding the magnetic properties of undoped Sr_2YRuO_6 .

Earlier, an attempt was made to explain the smallness of T_N by frustration effects in the Ising model, but the suppression of T_N in the Ising model proved to be too weak [8]. In this paper, we show that the major contribution is made by fluctuations of transverse spin components in the Heisenberg model. If only the nearest neighbors are taken into account, the antiferromagnetic state is unstable in the spin-wave approximation. Its stabilization requires including exchange with the next-nearest neighbors I or anisotropy D . Our calculations show that very small $I/J \sim D/J \sim 10^{-3}$ values are sufficient for obtaining the observed T_N and magnetic moment values.

2. THE SPECIAL FEATURES OF THE STRUCTURE AND EXCHANGE INTERACTION IN Sr_2YRuO_6

As distinct from other ruthenates and cuprates, neighboring RuO_6 octahedra in Sr_2YRuO_6 do not share anions (Fig. 1). This justifies applying the cluster approach to the description of its magnetic structure. Similarly, the electronic structure of Sr_2YRuO_6 is well modeled in first-principles band calculations by a system of RuO_6 clusters, which form an FCC lattice [8]. From the magnetic point of view, the replacement of Ru^{5+} magnetic by Y^{3+} nonmagnetic ions is diamagnetic

substitution. The FCC lattice of spins in Sr₂YRuO₆ can therefore be treated as produced by diamagnetic dilution of spins in the SrRuO₃ perovskite to a 0.5 concentration of nonmagnetic vacancies, which are spatially ordered (Fig. 1b). The presence of vacancies considerably changes the exchange interaction between neighboring Ru spins. Whereas ferromagnetic exchange interaction is characteristic of SrRuO₃, strong competition between ferromagnetic and antiferromagnetic interactions is observed in Sr₂RuO₄ [11], Sr_{2-x}Ca_xRuO₄ exhibits a trend toward antiferromagnetism as x increases (see discussion in review [12]), and Sr₂YRuO₆ is characterized by strong antiferromagnetic interaction. It follows that exchange interactions in various ruthenates vary to a greater extent than in cuprates, where these interactions are always antiferromagnetic.

The reason for the diversity of exchange interactions in ruthenates is the special features of their electronic structure formed by the ($t_{2g} - p$)- π bonds. The orbital degeneracy of the t_{2g} states results in the presence of three intersecting bands at the Fermi level and the metallic state of undoped SrRuO₃ and Sr₂RuO₄. The estimation of correlation effects in SrRuO₃ and Sr₂RuO₄ shows that intermediate correlations $U \leq W$, where U is the Hubbard Coulomb parameter and $W = z|t|$ is the band half-width, occur in these compounds [12]. Because of the diamagnetic dilution in Sr₂YRuO₆, the nearest neighbor Ru-Ru hopping integral t is strongly suppressed, and the substance is in the mode of strong electron correlations with the dielectric ground state. In the zeroth approximation with respect to hopping t , we have a system of independent RuO₆ clusters.

Consider the electronic structure of the RuO₆ cluster. The crystal field splits the Ru $4d$ level into the t_{2g} and e_g sublevels. The p orbitals of oxygen participate in the $pd\pi$ and $pd\sigma$ bonds with Ru. A detailed calculation of molecular orbitals and their comparison with first-principles calculations by the linearized augmented plane wave method were performed in [8]; in this work, we only give the results necessary for analyzing exchange interactions. After the inclusion of intracluster $p-d$ Ru-O hoppings, we obtain the following cluster molecular orbitals: 13 nonbonding molecular orbitals $4 \times E_0(p_\sigma) + 9 \times E_0(p_\pi)$, 5 bonding orbitals $2 \times E_-(E_g) + 3 \times E_-(T_{2g})$, and 5 antibonding molecular orbitals $2 \times E_+(E_g) + 3 \times E_+(T_{2g})$. Here, E_0 are the ionic levels, and the energies of the bonding and antibonding terms are

$$\begin{aligned} E_\pm(E_g) &= 0.5\{E_0(p_\sigma) + E_0(e_g) \\ &\pm [(E_0(p_\sigma) - E_0(e_g))^2 + 16t_\sigma^2]^{1/2}\}, \\ E_\pm(T_{2g}) &= 0.5\{E_0(p_\pi) + E_0(t_{2g}) \\ &\pm [(E_0(p_\pi) - E_0(t_{2g}))^2 + 16t_\pi^2]^{1/2}\}. \end{aligned} \quad (1)$$

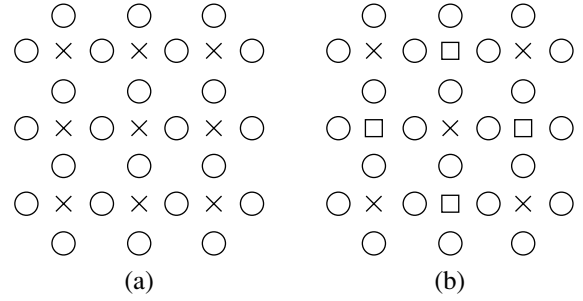


Fig. 1. Ordered diamagnetic replacement of every second Ru ion by Y ion in (a) SrRuO₃ leads to (b) the Sr₂YRuO₆ lattice: (x) Ru; (o) O; (□) Y.

The order of the levels is determined by the conditions

$$E_-(T_{2g}) \approx E_-(E_g) < E_0(p_\sigma) < E_0(p_\pi) < E_+(T_{2g}) < E_+(E_g),$$

and their filling with 39 valence electrons is such that 36 electrons completely fill the $E_-(T_{2g})$, $E_-(E_g)$, $E_0(p_\sigma)$, and $E_0(p_\pi)$ molecular orbitals. The remaining three electrons fill three $E_+(T_{2g})$ orbitals with parallel spins to form the $S = 3/2$ high-spin state. T_{2g} symmetry of molecular orbitals coincides with t_{2g} symmetry of Ru atomic orbitals.

The true crystal lattice of Sr₂YRuO₆ is somewhat more complex than that shown in Fig. 1; RuO₆ clusters are rotated through $\varphi \approx 12^\circ$, which results in $P21/n$ monoclinic symmetry. We will, however, analyze exchange interactions in terms of the undistorted structure (Fig. 1). Including distortions gives corrections which prove to be small according to the estimates made in [8]. From the point of view of the indirect exchange mechanism, exchange between the nearest neighbors J is formed by the Ru-O-O-Ru coupling. However, in terms of molecular orbitals, the same coupling of neighboring RuO₆ clusters is effected by the xy - xy hopping with the amplitude $\tau_\sigma = 0.75t_{dd\sigma}$.

The arising exchange energy per cluster can be estimated as $2J_0 \sim \tau_\sigma^2/\Delta$, where Δ is the exchange splitting of the T_{2g} molecular orbitals. The estimation of the τ_σ and Δ parameters by linearized augmented plane wave calculations in [8] gives $2J_0 \approx 0.05$ eV; this J value also corresponds to the energy difference between the ferromagnetic and antiferromagnetic states per cluster in spin polarization calculations [8], which equals 0.095 eV with and 0.12 eV without allowance for octahedron turns.

The magnetic properties of a system of localized spins will be described in terms of the isotropic Heisenberg model with the Hamiltonian

$$\begin{aligned} H &= -\frac{1}{2} \sum_{f,R} J(R) \mathbf{S}_f \cdot \mathbf{S}_{f+R}, \\ J(\mathbf{R}) &= J(-\mathbf{R}), \quad J(0) = 0. \end{aligned} \quad (2)$$

The FCC lattice contains $z = 12$ nearest neighbors with the exchange $J(\mathbf{R}_1) = -J$. We also take into account exchange with the next-nearest spins $J(\mathbf{R}_2) = I$ on the assumption of ferromagnetic exchange. Exchange for the next-nearest spins arises as the Ru–O–O–Ru–O–O–Ru coupling; it can be estimated as

$$I \sim \tau_G^4 / \Delta^3 \leq 10^{-2} J_0.$$

In order to describe the antiferromagnetic state, we introduce sublattices A (sites α) with spins upward and B (sites β) with spins downward, $\langle S_A^z \rangle = -\langle S_B^z \rangle \equiv \mathbf{S}$, where the magnetization of the sublattices depends on temperature. For the antiferromagnetic state of the first type, we have ferromagnetically ordered xy planes with an antiferromagnetic alternation of the planes. Set lattice parameter $a = 1$; the length of the $\mathbf{R}_1 \equiv \mathbf{\Delta}$ vectors connecting the nearest neighbors is then $\Delta = 1/\sqrt{2}$, and that of the $\mathbf{R}_2 \equiv \mathbf{a}$ vectors, $a = 1$. Let us divide the $\mathbf{\Delta}$ vectors into two groups, those lying in the xy planes \mathbf{d} and interplanar vectors $\mathbf{\delta}$,

$$\mathbf{d} = \left(\pm \frac{1}{2}, \pm \frac{1}{2}, 0 \right) (xy),$$

$$\mathbf{\delta}_1 = \left(0, \pm \frac{1}{2}, \pm \frac{1}{2} \right) (yz), \quad \mathbf{\delta}_2 = \left(\pm \frac{1}{2}, 0, \pm \frac{1}{2} \right) (xz).$$

The distribution of the $\langle S_f^z \rangle$ means in this model is as follows:

$$\begin{aligned} \langle S_\alpha^z \rangle &= \mathbf{S}, & \langle S_{\alpha+\mathbf{d}}^z \rangle &= \mathbf{S}, & \langle S_{\alpha+\mathbf{\delta}}^z \rangle &= -\mathbf{S}, \\ \langle S_{\alpha+\mathbf{a}}^z \rangle &= \mathbf{S}, & \langle S_\beta^z \rangle &= -\mathbf{S}, & \langle S_{\beta+\mathbf{d}}^z \rangle &= -\mathbf{S}, \\ \langle S_{\beta+\mathbf{\delta}}^z \rangle &= \mathbf{S}, & \langle S_{\beta+\mathbf{a}}^z \rangle &= -\mathbf{S}. \end{aligned} \quad (3)$$

Because of the ferromagnetic order in the xy plane, all four antiferromagnetic bonds in this plane are frustrated (energetically unfavorable). Eight interplanar antiferromagnetic bonds, however, give energy gain for the antiferromagnetic state. For this reason, frustrations decrease the mean field acting on a spin even in the molecular field approximation. Without frustrations, the mean field is $\bar{h} = 2J\bar{S} = 12J\bar{S}$; taking frustrations into account makes it $\bar{h} = 4J\bar{S}$. Without frustrations in the mean-field approximation, $T_N^{MF} = zJS(S+1)/3$, which is much higher than the experimental T_N value. A decrease in T_N by a factor of 3 caused by frustrations in the mean-field approximation does not solve the problem. A similar result is obtained for the Ising model, where frustrations decrease T_N [13]. The T_N value (700–900 K [8]) is, however, as previously, high compared with the experimental one. In the next section, we consider the spin-wave theory of a frustrated antiferromagnet to take into account transverse spin component fluctuations.

3. THE SPIN-WAVE THEORY OF A FRUSTRATED ANTIFERROMAGNET ON AN FCC LATTICE

The exact equation of motion ($\hbar = 1$) for S_f^+ is linearized in the Tyablikov approximation:

$$i\dot{S}_f^+ \approx \sum_{\mathbf{R}} J(\mathbf{R}) (\langle S_{f+\mathbf{R}}^z \rangle S_f^+ - \langle S_f^z \rangle S_{f+\mathbf{R}}^+). \quad (4)$$

The $h = H/zJ$ dimensionless Hamiltonian can conveniently be used. For the antiferromagnetic state of the first type, taking into account (3) then allows (4) to be written as ($\lambda = I/J$)

$$\begin{aligned} i\dot{S}_\alpha^+ &= \frac{\bar{S}}{z} \left[\sum_{\mathbf{d}} (S_{\alpha+\mathbf{d}}^+ - S_\alpha^+) + \sum_{\mathbf{\delta}} (S_{\alpha+\mathbf{\delta}}^+ + S_\alpha^+) \right] \\ &\quad + \frac{\lambda \bar{S}}{2z_2} \sum_{\mathbf{a}} (S_\alpha^+ - S_{\alpha+\mathbf{a}}^+), \\ i\dot{S}_\beta^+ &= -\frac{\bar{S}}{z} \left[\sum_{\mathbf{d}} (S_{\beta+\mathbf{d}}^+ + S_\beta^+) + \sum_{\mathbf{\delta}} (S_{\beta+\mathbf{\delta}}^+ + S_\beta^+) \right] \\ &\quad - \frac{\lambda \bar{S}}{2z_2} \sum_{\mathbf{a}} (S_\beta^+ - S_{\beta+\mathbf{a}}^+). \end{aligned} \quad (5)$$

Performing the Fourier transform over the sublattices

$$S_A^+(\mathbf{q}) = \sqrt{2/N} \sum_{\alpha} S_\alpha^+ \exp(i\mathbf{q} \cdot \alpha),$$

$$S_B^+(\mathbf{q}) = \sqrt{2/N} \sum_{\beta} S_\beta^+ \exp(i\mathbf{q} \cdot \beta),$$

we obtain

$$\begin{aligned} i\dot{S}_A^+(\mathbf{q}) &= \bar{S}(\alpha_q S_A^+(\mathbf{q}) + \beta_q S_B^+(\mathbf{q})), \\ i\dot{S}_B^+(\mathbf{q}) &= -\bar{S}(\alpha_q S_B^+(\mathbf{q}) + \beta_q S_A^+(\mathbf{q})), \end{aligned} \quad (6)$$

where

$$\alpha_q = 0.33(1 + c_x c_y) + 0.5\lambda(1 - \gamma_q),$$

$$\beta_q = 0.33(c_x + c_y)c_z,$$

$$c_i = \cos(q_i/2), \quad i = x, y, z,$$

$$\gamma_q = 0.33(\cos q_x + \cos q_y + \cos q_z).$$

The thermodynamic properties will be calculated using two-time retarded commutator Green's functions at finite temperatures

$$\langle \langle S_F^+(\mathbf{q}) | S_G^-(\mathbf{-q}) \rangle \rangle_\omega = G_{FG}(\mathbf{q}, \omega).$$

Here, sublattice indices F and G take on two values, A and B . For simplicity, we will only consider the spin

$S = 1/2$. Of course, spin-wave theory also can be constructed for an arbitrary spin S , including $S = 3/2$ for Sr₂YRuO₆. Such a theory will, however, be fairly cumbersome, whereas the main results for \bar{S} and T_N will differ by unimportant multipliers of the $S(S+1)$ type. Equations of motion (6) allow us to easily obtain the corresponding Green's functions

$$G_{AA} = \frac{2\bar{S}(\omega + \bar{S}\alpha_q)}{D(\mathbf{q}, \omega)}, \quad G_{BB} = \frac{2\bar{S}(\omega - \bar{S}\alpha_q)}{D(\mathbf{q}, \omega)}, \quad (7)$$

$$G_{AB} = G_{BA} = -\frac{2\bar{S}^2\beta_q}{D(\mathbf{q}, \omega)},$$

$$D(q, \omega) = \omega^2 - \Omega_q^2, \quad \Omega_q = \bar{S}\varepsilon_q, \quad (8)$$

$$\varepsilon_q = (\alpha_q^2(\lambda) - \beta_q^2)^{1/2}.$$

Applying the standard procedure yields the spectral density

$$n_{AA}(\mathbf{q}, \omega) = -\frac{1}{\pi} \text{Im} G_{AA}(\mathbf{q}, \omega)$$

$$= \bar{S} \left[\left(1 + \frac{\alpha_q}{\varepsilon_q} \right) \delta(\omega - \Omega_q) \right]$$

and the transverse spin correlator

$$C_{AA}(q) = \langle S_A^+(q) S_A^-(q) \rangle$$

$$= \int_{-\infty}^{\infty} \frac{\exp(\omega/\tau)}{\exp(\omega/\tau) - 1} n_{AA}(\mathbf{q}, \omega) d\omega \quad (9)$$

$$= \bar{S} \left(1 + \frac{\alpha_q}{\varepsilon_q} \coth \frac{\Omega_q}{2\tau} \right).$$

Here, $\tau = T/zJ$ is the dimensionless temperature. For $S = 1/2$,

$$\frac{2}{N} \sum_q C_{AA}(q) = \frac{2}{N} \sum_q \langle S_\alpha^+ S_\alpha^- \rangle = \frac{1}{2} + \bar{S}, \quad (10)$$

and the equation for the order parameter \bar{S} therefore reads

$$\bar{S}(\tau) = \frac{1/2}{I(\tau)}, \quad I(\tau) = \frac{2}{N} \sum_q \frac{\alpha_q}{\varepsilon_q} \coth \frac{\bar{S}(\tau)\varepsilon_q}{2\tau}. \quad (11)$$

At $\tau = 0$, the hyperbolic cotangent equals one, and

$$\bar{S}(0) = \frac{0.5}{I_1(\lambda)}, \quad I_1(\lambda) = 2N^{-1} \sum_q \frac{\alpha_q(\lambda)}{\varepsilon_q(\lambda)}. \quad (12)$$

In the other limit $\tau \rightarrow \tau_N$, $\bar{S} \rightarrow 0$ ($\coth x \rightarrow 1/x$ as

$x \rightarrow 0$), Eq. (11) yields the Néel temperature

$$\tau_N = \frac{1}{4} I_2(\lambda), \quad I_2(\lambda) = 2N^{-1} \sum_q \frac{\alpha_q(\lambda)}{\varepsilon_q^2(\lambda)}. \quad (13)$$

Consider the integrands in the expressions for I_1 and I_2 in the neighborhood of the Brillouin zone points $\Gamma = (0, 0, 0)$ and $X = (0, 0, 2\pi)$. In the neighborhood of Γ , we have

$$\alpha_q \approx \frac{1}{3} \left[2 - \frac{q_x^2 + q_y^2}{8} + \frac{\lambda q^2}{4} \right], \quad q^2 = q_x^2 + q_y^2 + q_z^2,$$

$$\beta_q \approx \frac{1}{3} \left[2 - \frac{q_x^2 + q_y^2}{8} - \frac{q_z^2}{4} \right], \quad \varepsilon_q^2 = \frac{q_z^2 + \lambda q^2}{9}$$

and the integrand in I_1 takes the form

$$\frac{\alpha_q(\lambda)}{\varepsilon_q(\lambda)} = \frac{2 - (q_x^2 + q_y^2)/8 + \lambda q^2/4}{(q_z^2 + \lambda q^2)^{1/2}}. \quad (14)$$

If only exchange J between the nearest neighbors is taken into account, the $\lambda = 0$ spectrum in the vicinity of Γ becomes one-dimensional with the special direction z , along which A and B layer spins alternate. At $\lambda = 0$, the integral I_1 logarithmically diverges, which means that $\bar{S}(0) \rightarrow 0$; that is, the antiferromagnetic state is already unstable at $T = 0$. The integral I_2 in the vicinity of Γ behaves as $\int dq_z/q_z^2 \propto 1/q$, that is, diverges by a power law. As a result, $T_N \rightarrow 0$. In the vicinity of X , the I_1 and I_2 integrals exhibit similar behaviors. It follows that, if only nearest neighbor exchange J is taken into account, the effect of frustrations is strong to the extent that the antiferromagnetic state is completely suppressed. Precisely this is, in our view, the main reason why T_N and \bar{S} are small in Sr₂YRuO₆. The antiferromagnetic state can be stabilized both by exchange with the next-nearest spins I and by anisotropy.

4. THE STABILIZATION OF ANTIFERROMAGNETIC STATES BY NEXT-NEAREST-NEIGHBOR EXCHANGE

The instability of the antiferromagnetic state in FCC lattices has long been known and treated within the frameworks of both the spin-wave approach and the Bete–Peierls–Weiss cluster approximation [14–16]. The stabilization of the antiferromagnetic state by next-nearest-neighbor exchange has been considered in detail in [17, 18]. Ferromagnetic exchange I stabilizes the antiferromagnetic phase of the first type, which is observed in Sr₂YRuO₆, and antiferromagnetic exchange I stabilizes the phase of the third type. The Néel temperature as a function of the $\lambda = I/J$ ratio was calculated in [17, 18] only numerically, and the $T_N(\lambda)$ plots with a characteristic nonanalytic dependence for

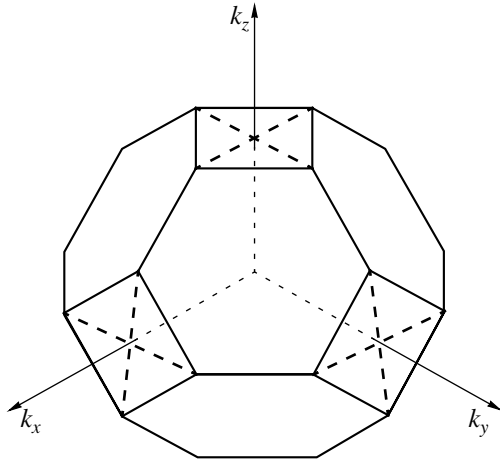


Fig. 2. Brillouin zone of a face-centered cubic lattice. Squares indicate dangerous directions leading to magnetic moment and Néel temperature divergences.

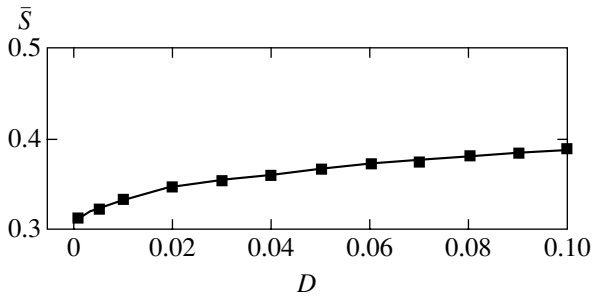


Fig. 3. Dependence of sublattice magnetic moment \bar{S} on exchange anisotropy D .

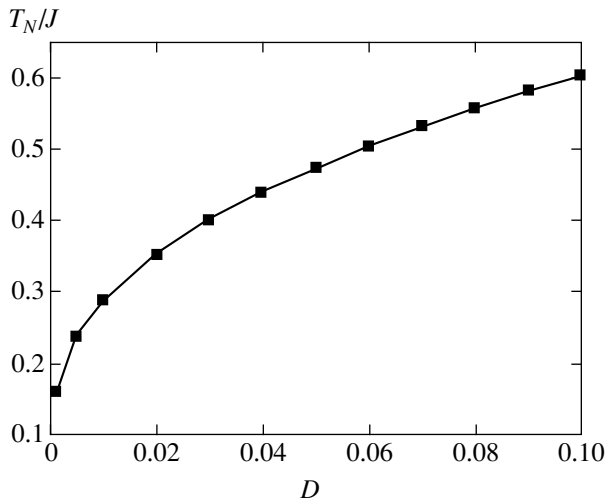


Fig. 4. Dependence of the Néel temperature on exchange anisotropy D .

$\lambda \rightarrow 0$ were similar to the $T_N(D)$ plot (see Fig. 4 below). At the same time, it was claimed in [17, 18] that anisotropy of exchange interactions per se, without taking exchange I into account, could not stabilize the anti-

ferromagnetic state of the first type. This conclusion is at variance with our results. Indeed, anisotropy creates a gap in the spectrum of magnons that cuts off the divergences as λ tends to 0. This problem is considered in more detail in the next section.

5. THE STABILIZATION OF THE ANTIFERROMAGNETIC STATE BY ANISOTROPY

The turns of the octahedra and the monoclinic distortion of the Sr_2YRuO_6 lattice can cause anisotropy of two types, namely, single-ion anisotropy of the DS_z^2 type or exchange coupling anisotropy. In our simplified model with $S = 1/2$, the single-ion anisotropy is absent; therefore, consider the exchange anisotropy. The Hamiltonian of the system can then be written as

$$H = -\frac{1}{2} \sum_{f, R} J(R) (S_f^+ S_{f+R}^- + \xi_R S_f^z S_{f+R}^z), \quad \xi_R \neq 1.$$

Equation (4) now transforms into

$$iS_f^+ \approx \sum_R J(\mathbf{R}) (\xi_R \langle S_{f+R}^z \rangle S_f^z - \langle S_f^z \rangle S_{f+R}^+).$$

In the simplest situation, it suffices to take into account exchange anisotropy for the nearest neighbors ignoring exchange anisotropy for the next-nearest spins. This implies that

$$\xi_\Delta = 1 + D, \quad \xi_a = 1,$$

where D is the dimensionless anisotropy parameter. As the lattice distortions are small, we can assume that $D \ll 1$. The spin-wave theory described in Section 3 can easily be generalized to systems with anisotropy. After the $\alpha_q \rightarrow \alpha_q(D)$ renormalization,

$$\alpha_q(\lambda, D) = 0.33(1 + D + c_x c_y) + 0.5\lambda(1 - \gamma_d), \quad (15)$$

$$\varepsilon_q(D) = (\alpha_q^2(\lambda, D) - \beta_q^2)^{1/2},$$

all the other equations obtained in Section 3 remain valid. The order parameter at $T = 0$ is

$$\bar{S}(\lambda, D) = \frac{0.5}{I_1(\lambda, D)}, \quad (16)$$

$$I_1(\lambda, D) = \frac{2}{N} \sum_q \frac{\alpha_q(\lambda, D)}{\varepsilon_q(\lambda, D)}.$$

For the Néel temperature, we obtain

$$\tau_N(\lambda, D) = \frac{0.25}{I_2(\lambda, D)}, \quad (17)$$

$$I_2(\lambda, D) = \frac{2}{N} \sum_q \frac{\alpha_q(\lambda, D)}{\varepsilon_q^2(\lambda, D)}.$$

If $\lambda = 0$ and $D \rightarrow 0$, both integrals I_1 and I_2 diverge, which yields $\bar{S} = 0$ and $\tau_N = 0$. It follows that anisotropy per se, in the absence of next-nearest-neighbor spin exchange, stabilizes the antiferromagnetic state in an FCC lattice.

To single out the diverging asymptotic functions, we analytically calculated the contributions to the integrals in the neighborhood of the dangerous Brillouin zone points Γ and X (see Fig. 2). The high-symmetry points will be denoted as follows:

$$\Gamma(0, 0, 0), \quad L = (\pi, \pi, \pi), \quad K = (3\pi/2, 3\pi/2, 0)$$

$$Z(0, 0, 2\pi), \quad W_1(\pi, 0, 2\pi), \quad W_2 = (0, \pi, 2\pi),$$

$$X = (2\pi, 0, 0), \quad \tilde{W}_1 = (2\pi, \pi, 0), \quad \tilde{W}_2 = (2\pi, 0, \pi),$$

$$Y = (0, 2\pi, 0), \quad W_1^* = (\pi, 2\pi, 0), \quad W_2^* = (0, 2\pi, \pi).$$

Along several Brillouin zone directions shown by squares in Fig. 2, $\varepsilon_q = 0$ at $D = \lambda = 0$. Some points of this set are dangerous in the sense that the I_1 and I_2 integrals diverge at $D = \lambda = 0$. Further, we will study the role played by anisotropy D on the assumption $\lambda = 0$.

Consider the small volume $v = (\pi/4)^3$ in the neighborhood of Γ (recall that the total Brillouin zone volume is $32\pi^3$). All integrals normalized with respect to v will be denoted by \tilde{I} . Expanding all cosines into series and performing fairly simple calculations, we can analytically find the contributions that diverge as $D \rightarrow 0$. For instance, for I_1 , we obtain

$$\tilde{I}_1(D) \approx 0.5 \ln D - 1.9.$$

For the integral \tilde{I}_2 , analytic calculations give

$$\tilde{I}_2(D) \approx 12/\sqrt{D}.$$

Similar asymptotic behaviors ($\ln D$ for I_1 and \sqrt{D} for I_2) can also be obtained for the other dangerous Brillouin zone points. As a result, we find $\bar{S}(D)$ and $T_N(D)/J$.

The $\bar{S}(D)$ and $T_N(D)/J$ dependences at $\lambda = 0$ are shown in Figs. 3 and 4. The curves labeled by squares are described by the approximations

$$\bar{S}(D) \approx \frac{1/2}{0.043 \ln D + 1.256}, \quad (18)$$

$$T_N(D) = J \begin{cases} 4\sqrt{D}/(1 + 4\sqrt{D}), & 0 < D < 0.05, \\ 0.342 + 2.6D, & 0.05 < D < 0.1. \end{cases} \quad (19)$$

6. RESULTS AND DISCUSSION

Our results are based on a study of the Tyablikov approximation, which is, in essence, a mean-field

approximation variant. However, as distinct from the trivial Weiss mean field with $J_{ij}\mathbf{S}_i\mathbf{S}_j \rightarrow J_{ij}\langle S_i^z \rangle S_j^z$, which does not depend on the space dimension, the Tyablikov approximation takes into account transverse spin density fluctuations in the form of collective excitations, that is, spin waves. As a result, the Tyablikov approximation reveals the absence of long-range order at finite temperatures in agreement with the exact Mermin–Wagner theorem [17, 18]. As long as there is long-range magnetic order in the system and spin fluctuations at low temperatures can be described in terms of spin waves, we can hope that the results obtained using the Tyablikov approximation will be in at least qualitative agreement with experiment.

Note that the stabilization of the antiferromagnetic state of the first type takes place not at arbitrary signs of exchange and anisotropy, but only at ferromagnetic next-nearest-neighbor exchange I and anisotropy $D > 0$. Indeed, ferromagnetic exchange I prevents frustrations and is intrasublattice. Conversely, antiferromagnetic next-nearest-neighbor exchange would only strengthen the effect of frustrations. As far as anisotropy is concerned, $D > 0$ is evidence of Ising-type anisotropy, $J_{\parallel} > J_{\perp}$. In the limit $D \rightarrow \infty$, we can ignore transverse spin components and obtain the Ising model, for which frustrations partially suppress the antiferromagnetic phase, but T_N and \bar{S} remain finite [13]. At all $D > 0$ values, a gap appears in the spectrum of magnons, which is the factor that stabilizes the antiferromagnetic phase. At $D < 0$, the $\varepsilon_q(D)$ spectrum of magnons becomes imaginary at certain wave vectors, which is evidence of antiferromagnetic phase instability. At $D = 0$, the antiferromagnetic state with a long-range order is unstable and is replaced by a state with a spin-liquid-type short-range order [19, 20].

A comparison of our results with the experimental data on Sr₂YRuO₆ should be performed bearing in mind that the monoclinic distortion of the lattice and the spin $\bar{S} = 3/2$ can lead not only to exchange but also to single-ion anisotropy. The Dzyaloshinski–Moriya anisotropic exchange is also possible. Clearly, all anisotropic interactions are weak compared with J , which allows us to qualitatively compare our results with experiment taking into account exchange anisotropy with $D \ll J$ only. It follows from (18) and (19) that, to obtain $T_N = 30$ K and $J = 300$ K, we must set $D = 8 \times 10^{-4}$. This means that the exchange anisotropy $J_{\parallel} - J_{\perp} = D_j = 0.24$ K is exceedingly small. At such an anisotropy value,

$$\bar{S}(8 \times 10^{-4}) = 0.32,$$

which amounts to 64% of the nominal spin and very closely agrees with the neutron data on the magnetic moment of ruthenium.

Note in conclusion that frustrations in an FCC system with nearest neighbor exchange lead to soft mag-

non modes along several Brillouin zone directions. In particular, in the vicinity of the Γ point, the spectrum becomes one-dimensional. For this reason, divergences in spin-wave theory similar to divergences in low-dimensional systems are not surprising. Very weak perturbations in the form of ferromagnetic next-nearest-neighbor exchange or an Ising-type exchange anisotropy are sufficient for the antiferromagnetic state to be stabilized.

ACKNOWLEDGMENTS

One of the authors (S.G.O.) thanks the Naval Research Laboratory for financial support of his visit to the Department of the Theory of Complex Systems in August 2001, where this work was initiated, and I.I. Mazin and the other members of the department for hospitality.

This work was financially supported by the Russian Foundation for Basic Research (project no. 00-02-16110), RFFI-KKFN "Enisei" (project no. 02-02-97705), INTAS (grant 01-0654), and the Quantum Macrophysics Program of the Russian Academy of Sciences.

REFERENCES

1. Y. Maeno, H. Hasimoto, K. Yoshida, *et al.*, *Nature* **372**, 532 (1994).
2. S. Nakatsuji and Y. Maeno, *Phys. Rev. Lett.* **84**, 2666 (2000).
3. S. Nakatsuji and Y. Maeno, *Phys. Rev. B* **62**, 6458 (2000).
4. J. J. Randall and Ward, *J. Am. Chem. Soc.* **81**, 2629 (1959).
5. J. M. Longo, P. M. Raccah, and J. B. Goodenough, *J. Appl. Phys.* **39**, 1327 (1968).
6. P. D. Battle and W. J. Macklin, *J. Solid State Chem.* **54**, 245 (1984).
7. G. Cao, Y. Xin, C. S. Alexander, and J. E. Crow, *Phys. Rev. B* **63**, 184432 (2001).
8. I. I. Mazin and D. J. Singh, *Phys. Rev. B* **56**, 2556 (1997).
9. M. K. Wu, D. Y. Chen, F. Z. Chein, *et al.*, *Z. Phys. B* **102**, 37 (1997).
10. H. A. Blackstead, *Abstract of the International Conference on Modern Problems of Superconductivity*, Yalta, Ukraine (2002).
11. I. I. Mazin and D. J. Singh, *Phys. Rev. Lett.* **82**, 4324 (1999).
12. S. G. Ovchinnikov, *Usp. Fiz. Nauk* **173**, 27 (2003).
13. R. Liebmann, *Statistical Mechanics of Periodic Frustrated Ising Systems* (Springer, Berlin, 1986).
14. Y. Y. Li, *Phys. Rev.* **84**, 721 (1951).
15. J. M. Ziman, *Proc. R. Soc. London, Ser. A* **66**, 89 (1953).
16. D. ter Haar and M. E. Lines, *Philos. Trans. R. Soc. London, Ser. A* **255**, 1 (1962).
17. M. E. Lines, *Proc. R. Soc. London* **271**, 105 (1963).
18. M. E. Lines, *Phys. Rev. A* **135**, 1336 (1964).
19. H. Shimara and S. Takida, *J. Phys. Soc. Jpn.* **60**, 2394 (1991).
20. A. Barabanov and O. Starykh, *J. Phys. Soc. Jpn.* **61**, 704 (1992).

Translated by V. Sipachev